Improved Homogenization of Ni in Sintered Steels through the Use of Cr-Containing Prealloyed Powders

M.W. WU and K.S. HWANG

The homogenization of Ni in powder metal (PM) steel compacts is usually difficult even after high-temperature sintering at 1250 °C. An earlier study by the authors demonstrated that this problem can be alleviated through the addition of 0.5 wt pct Cr in the form of stainless steel powders. To further improve the microstructure and mechanical properties of Ni-containing PM steels and to understand the mechanisms, an attempt was made in this study using the Fe-3Cr-0.5Mo prealloyed powder as the base material. The results showed that the distribution of the Ni additives was significantly improved. As a result, the tensile strength of the Fe-3Cr-0.5Mo-4Ni-0.5C compact sintered at 1250 °C reached 1323 MPa. The elongation was higher than 1 pct. These sinter-hardened properties, which were attained using a slow furnace cooling rate, were comparable to those of the sinter-hardened alloys reported in the literature using accelerated cooling and were equivalent to those of the best quenched-and-tempered alloys registered in the Metal Powder Industries Federation (MPIF) standards. These improvements were attributed to the positive effect of Cr addition on alloy homogenization due to the reduction of the repelling effect between Ni and C, as was demonstrated through the thermodynamic analysis using the Thermo-Calc program.

I. INTRODUCTION

NICKEL, Cu, and Mo are the most frequently used alloying elements in powder metal (PM) steel products. Among these three elements, Ni has the slowest diffusion rate into iron, and thus the full benefits of Ni alloying are lost. As a result, heterogeneous microstructures and insufficiently satisfactory mechanical properties are often found in sintered Ni-containing steels, such as in diffusion-alloyed FD-0405 (Fe-4Ni-1.5Cu-0.5Mo-0.5C) and sinter-hardened FLN4-4408 (Fe-4Ni-0.8Mo-0.75C), which are the standard materials contained in the Metal Powder Industries Federation (MPIF) standards.[1] These Ni-containing steel compacts usually consist of pearlite, bainite, martensite, and a substantial amount of Ni-rich areas.[2,3] The Ni-rich areas were found to be lean in carbon and were soft and were located at sintered necks or in pore-rich areas, which are the most vulnerable sites during mechanical testing.[3–7]

To improve the alloy and microstructure homogenization and the mechanical properties, elimination of the weak Ni-rich/C-lean areas is necessary. An intuitive approach to solving this problem is to use prealloyed steel powders. However, the poor compressibility of the hard prealloyed powder has prohibited its wide application. Another alternative is to employ smaller and more spherical Ni powders or to use Ni-coated iron powders.[8,9,10] The use of fine carbonyl iron powders, such as in the metal injection molding process, also provides sintered compacts a more homogenized microstructure due to the short diffusion distance.[9,10] The uniformity of Ni may also be influenced by other alloying additives. The effect of adding Mo and Cu has been shown to be insignificant, as was demonstrated by the inhomogeneous Ni distribution in sintered FD-0405 and FLN4-4408 compacts.[2,3,11] The carbon, on the other hand, has a negative effect because Ni and C tend to repel each other due to their high interaction energies.[12]

Because Cr is a strong carbide former, which could change the chemical potential of carbon in Ni-rich phases, it is possible that the presence of Cr would alleviate the repelling effect between Ni and C and help the Ni homogenization. However, the use of Cr as an alloying element is rare for regular PM industries. The difficulty comes from its high oxygen affinity. Thus, low dewpoint and high-temperature sintering are required to prevent the oxidation of Cr.[13] This problem can be alleviated by reducing the activity of Cr using Cr-containing prealloyed powders. Wu *et al.* reported that the amount of soft Ni-rich/C-lean areas in the Fe-4Ni-1.5Cu-0.5Mo-0.5C compact can be reduced when 0.5 wt pct Cr is introduced in the 316L stainless steel powder form.[2] The Cr addition helps homogenize Ni and C and promote the formation of martensite and bainite, and as a result, it improves the mechanical properties. However, the addition of the 3 wt pct stainless steel powder into iron powders also increases the amount of Ni by 0.38 wt pct Ni. This complicates the postulation of improving Ni homogenization by adding Cr. Moreover, the activity of Cr in the stainless steel powder is still high and the Cr still needs to be homogenized first in order to aid the Ni homogenization. Thus, using Cr-containing prealloyed powder as the base material and increasing the amount of Cr would be the next logical approaches to further attain the full benefit of the Ni alloying. The objective of this study was thus to investigate the microstructure homogenization and mechanical properties of the Fe-4Ni-3Cr-0.5Mo-0.5C compact using Fe-3Cr-0.5Mo prealloyed powder as the base material and to understand the rationale behind these improvements.

II. EXPERIMENTAL PROCEDURE

The base powder used in this study was a prealloyed powder that contained 3 wt pct Cr and 0.5 wt pct Mo. To

M.W. WU, Graduate Student, and K.S. HWANG, Professor, are with the Department of Materials Science and Engineering, National Taiwan University, Taipei, 106 Taiwan, Republic of China. Contact e-mail: kshwang@ccms.ntu.edu.tw

Manuscript submitted June 1, 2006.

this Fe-3Cr-0.5Mo powder, designated as FeCrMo powder in this study, were added 4 wt pct Ni elemental powders. In order to separate the effect of 3 wt pct Cr in the FeCrMo powder on the homogenization of Ni, Fe-0.5Mo prealloyed steel powders were also used for comparison. The characteristics of the prealloyed powder and the elemental Ni powder are summarized in Table I.

To prepare the specimens, the prealloyed powder was mixed with 0.8 wt pct zinc stearate and 0.5, 0.6, and 0.7 wt pct graphite, respectively, in a V-cone mixer for 30 minutes. The admixed powder was compacted into tensile bars per MPIF standard 10 at a pressure of about 550 MPa. The green densities thus attained were 6.85 g/cm^3. The green specimens were then held at 550 °C for 15 minutes to remove the lubricant and were subsequently sintered at 1120 °C for 30 minutes or at 1250 °C for 60 minutes in a tube furnace. Both debinding and sintering were performed in an atmosphere of N_2-9 pct H_2. The dewpoint of the atmosphere was below −45 °C. The cooling rate of the specimen after sintering was about 0.1 °C/s at 550 °C.

The densities of the sintered compacts were measured using the Archimedes' method. Tensile tests were performed using a strain rate of 0.0224/min. The apparent hardness was tested mainly using a Rockwell C scale. However, when the hardness was lower than HRC20, a Rockwell B scale was used instead. For microhardness measurements, the Vickers hardness was used with a loading of 0.098 N. The data reported were averages of eight specimens. For microstructure observations, sintered tensile bars were ground, polished, and etched with a mixed solution of 2 pct Nital and 4 pct Picral. The microstructures and fracture surfaces were examined under an optical microscope or a scanning electron microscope (SEM, XL-30, Philips, Eindhoven, Holland). An electron probe microanalyzer (EPMA, JXA-8600SX, JEOL, Tokyo) was used to investigate the distribution of the alloying elements. To identify the locations and phases where the fracture occurred, a sintered Fe-0.5Mo-4Ni-0.5C compact, in which the Ni was not homogenized, was examined inside an SEM. Photos were taken, before and after fracturing, over the regions with the smallest cross-sectional area. A comparison was then made to identify the crack paths.

In order to verify the role of Cr in the homogenization of microstructures, the Thermo-Calc program and a TCFE3 database (Thermo-Calc Software, Stockholm) were used to calculate the chemical potential of carbon in the Fe-3Cr-0.5Mo-0.5C-xNi, Fe-0.5Mo-0.5C-xNi, and Fe-0.5C-xNi steel compacts sintered at 1120 °C. The results were used to explain the difference in microstructure and Ni distribution in sintered compacts with and without Cr.

III. RESULTS AND DISCUSSION

A. *Sintered Density and Carbon Content*

Table II shows the densities and carbon contents of the FeCrMo and FeCrMo-4Ni compacts after sintering at 1120 °C and 1250 °C. The data show that the sintered densities increased with increasing sintering temperature and Ni content. Such enhanced densification caused by the Ni addition agreed with those reported in the literatures.[9,10] The combined carbon contents were all lower than the amounts of graphite added by about 0.1 wt pct due to decarburization. The carbon content did not have much influence on the sintered densities of either the FeCrMo or FeCrMo-4Ni alloys.

B. *Mechanical Properties*

1. *Strength and hardness*

The mechanical properties of the sintered compacts investigated in this study are listed in Table III. The apparent hardnesses and tensile strengths of the FeCrMo compacts sintered at 1120 °C were from HRB 82.3 to 86.3 and from 474 to 611 MPa, respectively, depending on the carbon content. When the sintering temperature was increased to 1250 °C, the properties improved only slightly. This was because the Cr and Mo had already been homogenized in the prealloyed powder. The high-temperature sintering did not help in this regard. Instead, the high temperature actually lowered the carbon content. Thus, the increase in tensile strength was mainly due to the slight increase in sintered density and possibly also due to the pore rounding effect.

However, when 4 wt pct Ni was added, the mechanical properties were significantly improved, particularly for

Table I. Characteristics of the Prealloyed Fe-3Cr-0.5Mo and Fe-0.5Mo Steel Powders and Elemental Ni Powders Used in This Study

Type	Fe-3Cr-0.5Mo	Fe-0.5Mo	Ni
Designation	CrM	ATOMET 4001	Ni-123
Average particle size	D_{10} = 17.7 μm D_{50} = 70.9 μm D_{90} = 121.1 μm	D_{10} = 31.4 μm D_{50} = 72.9 μm D_{90} = 161.7 μm	D_{10} = 2.4 μm D_{50} = 3.7 μm D_{90} = 6.9 μm
Apparent density, g/cm^3	2.90 (Hall density)	2.93 (Hall density)	2.04 (Arnold density)
Flow rate, s/50 g	25	26.1	—
Chemistry			
C, wt pct	0.003	0.004	0.079
O, wt pct	0.21	0.08	0.208
Mo, wt pct	0.5	0.497	—
Cr, wt pct	3.0	—	—
Mn, wt pct	—	0.131	—
Supplier	Höganäs	QMP	Inco

Table II. Densities and Carbon Contents of the Sintered Fe-3Cr-0.5Mo-*x*C and Fe-3Cr-0.5Mo-4Ni-*x*C Compacts

Composition	Graphite Added (Wt Pct)	Sintering Temperature (°C)	Sintered Density (g/cm^3)	Carbon Content (Wt Pct)
Fe-3Cr-0.5Mo-0.4C	0.5	1120	6.88	0.42
Fe-3Cr-0.5Mo-0.4C	0.5	1250	6.94	0.39
Fe-3Cr-0.5Mo-0.5C	0.6	1120	6.88	0.51
Fe-3Cr-0.5Mo-0.5C	0.6	1250	6.92	0.49
Fe-3Cr-0.5Mo-0.6C	0.7	1120	6.85	0.62
Fe-3Cr-0.5Mo-0.6C	0.7	1250	6.95	0.60
Fe-3Cr-0.5Mo-0.4C-4Ni	0.5	1120	7.05	0.41
Fe-3Cr-0.5Mo-0.4C-4Ni	0.5	1250	7.23	0.38
Fe-3Cr-0.5Mo-0.5C-4Ni	0.6	1120	7.05	0.50
Fe-3Cr-0.5Mo-0.5C-4Ni	0.6	1250	7.23	0.49
Fe-3Cr-0.5Mo-0.6C-4Ni	0.7	1120	7.06	0.62
Fe-3Cr-0.5Mo-0.6C-4Ni	0.7	1250	7.24	0.59

Table III. Mechanical Properties of the As-Sintered Fe-3Cr-0.5Mo-*x*C with the Addition of Elemental Ni Powders

Composition	Sintering Temperature (°C)	Hardness, HRC or **HRB** (HV)	Tensile Strength (MPa)	Elongation (Pct)
Fe-3Cr-0.5Mo-0.4C	1120	**82.3** (157)	474	1.5
Fe-3Cr-0.5Mo-0.4C	1250	**82.9** (159)	552	2.0
Fe-3Cr-0.5Mo-0.5C	1120	**86.3** (170)	611	1.5
Fe-3Cr-0.5Mo-0.5C	1250	**88.5** (178)	651	1.7
Fe-3Cr-0.5Mo-0.6C	1120	**85.7** (168)	602	1.3
Fe-3Cr-0.5Mo-0.6C	1250	**84.2** (163)	665	1.4
Fe-3Cr-0.5Mo-0.4C-4Ni	1120	27.8 (284)	849	1.6
Fe-3Cr-0.5Mo-0.4C-4Ni	1250	37.4 (367)	1237	1.8
Fe-3Cr-0.5Mo-0.5C-4Ni	1120	28.9 (293)	859	1.6
Fe-3Cr-0.5Mo-0.5C-4Ni	1250	39.2 (385)	1323	1.8
Fe-3Cr-0.5Mo-0.6C-4Ni	1120	26.6 (275)	807	1.8
Fe-3Cr-0.5Mo-0.6C-4Ni	1250	32.8 (323)	1032	2.1

compacts containing 0.4 or 0.5 wt pct carbon. When the amount of the combined carbon increased to 0.6 wt pct, the mechanical properties deteriorated because of the presence of retained austenite, which will be explained later. The highest hardness and tensile strength were attained with FeCrMo-4Ni-0.5C and were HRC39.2 and 1323 MPa, respectively. The strength was higher than twice that obtained with the FeCrMo-0.5C without the 4 wt pct Ni addition. As shown in Table IV, these properties are much better than those of the as-sintered or sinter-hardened high-strength PM steels, as reported in recent literature or in the MPIF standards.[1,2,11,14–17] Moreover, the 1323 MPa obtained without quenching heat treatment or accelerated cooling is equivalent to the best tensile strength of the quenched and tempered materials registered in the MPIF standards, *i.e.,* FLN2-4405-190HT.[1] These results showed that the Cr addition is very effective in improving the mechanical properties of Ni-containing materials. The effect of Cr addition can also be examined by comparing these properties with those of Fe-0.5Cr-0.5Mo-4Ni-1.5Cu-0.5C, as reported by Wu *et al.* recently.[2] Because the amount of Mo and Ni are similar, the improvements in mechanical properties attained in this study must be attributed to the increase of the Cr from 0.5 to 3 wt pct.

The effect of the cooling rate can also be revealed from the data of Fe-3Cr-0.5Mo-0.6C with a density of about 7.0 g/cm^3, as shown in Table IV. With a faster cooling rate of 0.8 °C/s, the tensile strength reached 1291 MPa,[14] which is about twice the 665 MPa obtained in this study with a cooling rate of 0.1 °C/s. This suggests that the 1323 MPa tensile strength of the FeCrMo-4Ni-0.5C material of this study can be further enhanced if the current furnace cooling process, which has a cooling rate of about 0.1 °C/s at 550 °C, is changed to the forced cooling process, such as that used in the industrial practices for sinter hardening materials.

2. *Ductility*

In addition to the excellent tensile strength and hardness, the elongations of the FeCrMo-4Ni-xC compacts were all greater than 1.0 pct. The typical fracture surfaces were the ductile type, as shown in Figure 1. These ductility results indicated that these materials are suitable for structural parts applications. In contrast, most, if not all, sintered steels that have a comparable tensile strength and hardness are with an elongation less than 1 pct.[1]

Further, note in Table III that when the tensile strength and hardness increased, the elongation also increased. This was mainly attributed to the density increase when the sintering temperature increased or when 4 wt pct Ni was added. Another reason was that the density increase helped enlarge the load-bearing neck area. The high sintering temperature also caused pore rounding, which reduced the stress concentration effect and thus increased the ductility of the alloys.

Table IV. Comparison of the Mechanical Properties and Processing Conditions of Some Sinter-Hardened Steel Compacts Reported in the Literature[1,2,11,14-17]

Composition	Reference	Sintering Temperature (°C)	Sintered Density (g/cm^3)	Cooling Rate (°C/S)	Ultimate Tensile Strength (MPa)	Processing Condition
Fe-3Cr-0.5Mo-4Ni-0.5C	this study	1250	7.23	0.1	1323	sintered and tempered
Fe-3Cr-0.5Mo-0.5C	this study	1250	6.92	0.1	651	sintered and tempered
Fe-3Cr-0.5Mo-0.6C	this study	1250	6.95	0.1	665	sintered and tempered
Fe-1.2Mo-1.5Ni-2Cu-0.4Mn-0.8C (FLC2-4808)	MPIF[1]	—	7.20	—	1070	sintered and tempered
Fe-0.8Mo-2Ni-2Cu-0.8C (FLNC-4408)	MPIF[1]	—	7.20	—	970	sintered and tempered
Fe-0.5Mo-2Ni-2Cu-0.5C (FD-0405)	MPIF[1]	—	7.35	—	850	as-sintered
Fe-1.5Mo-4Ni-2Cu-0.2Mn-0.5C (FLDN4C2-4905)	MPIF[1]	—	7.35	—	970	as-sintered
Fe-0.5Mo-4Ni-0.2Mn-1.5Cu-0.5C (FLN4C-4005)	MPIF[1]	—	7.40	—	970	as-sintered
Fe-2Ni-1.25Cu-0.75C (FN-0208-155HT)	MPIF[1]	—	7.2	—	1170	quenched and tempered
Fe-2Ni-0.8Mo-0.55C (FLN2-4405-190HT)	MPIF[1]	—	7.2	—	1338*	quenched and tempered
Fe-0.5Mo-4Ni-1.5Cu-0.5C	Wu et al.[2]	1250	7.00	0.1	626	sintered and tempered
Fe-0.5Mo-4Ni-1.5Cu-0.5Cr-0.5C	Wu et al.[2]	1250	7.06	0.1	801	sintered and tempered
Fe-3Cr-0.5Mo-0.6C	Marcu et al.[14]	1250	7.01	0.8	1291	sintered and tempered
Fe-3Cr-0.5Mo-0.6C	Marcu et al.[14]	1250	7.19	0.8	1361	sintered and tempered
Fe-3Cr-0.5Mo-0.4C	Hu et al.[15]	1250	7.30	2–3	1400	sintered and tempered
Fe-0.85Mo-4Ni-0.35Si-0.5C	Hanejko et al.[16]	1260	7.19	1	1250	sintered and tempered
Fe-0.85Mo-4Ni-0.70Si-0.5C	Hanejko et al.[16]	1260	7.09	1	1240	sintered and tempered
Fe-1.5Mo-3Si-1.2C	Youseffi et al.[17]	1250	7.55	0.33	764	sintered and tempered
Fe-0.85Mo-6Ni-0.4C	Gething et al.[11]	1288	7.50	—	943	as-sintered

*Estimated from those of 7.05 and 7.30 g · cm^3 compacts.

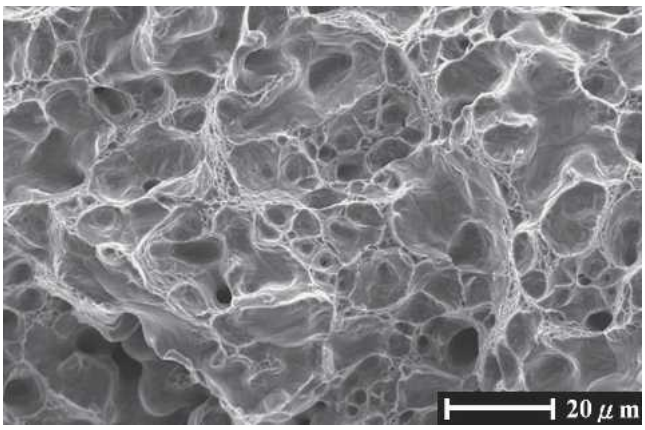

Fig. 1—The fracture surface of the Fe-3Cr-0.5Mo-4Ni-0.5C compact that was sintered at 1250 °C shows a ductile type of fracture.

C. *Microstructure and Distribution of Alloying Elements of FeCrMo-4Ni*

Figure 2 shows the microstructures of FeCrMo-0.5C compacts sintered at 1120 °C and 1250 °C. Both specimens contained mainly pearlite with some ferrite. When 4 wt pct Ni was added, the compact sintered at 1120 °C showed fine pearlite in the powder core and bainite or martensite in the surrounding areas, as shown in Figures 3(a) and (b). The hardnesses measured for bainite and martensite were about HV325 and HV435, respectively. A small amount of soft area with a microhardness of HV 228, which had no lamellae or featherlike features, as shown in Figure 3(a), was found with the Ni content above 11 wt pct. These areas were austenite and were present in pore-rich regions, as shown by the dot mapping of Ni in Figure 4. It was noticed that the soft Ni-rich ferrite with a hardness of about HV140, which was found in the powder periphery of Fe-0.5Mo-4Ni-1.5Cu-0.5C compacts reported by Wu *et al.,* did not appear here in the FeCrMo-4Ni-0.5C compact. Because both materials contained the same amount of Ni, Mo, and carbon, the difference in the microstructures, particularly the absence of weak Ni-rich areas, suggested that the Cr in the FeCrMo base powder must be the main reason enhancing the Ni homogenization.

When the sintering temperature was increased to 1250 °C, the compact consisted mainly of bainite and martensite, as illustrated in Figure 3(c). No pearlite, Ni-rich ferrite, or Ni-rich austenite was found. The homogenization of Ni was much improved due to the addition of Cr and the high-temperature sintering, as indicated by the dot mapping of Ni in Figure 5. Because pearlite could still be found easily in most Ni-containing PM steels, which were sintered at 1250 °C,[2] the improved Ni homogenization observed in Figure 3(c) must be mainly attributed to the Cr addition. It seemed that the Cr helped enhance the Ni

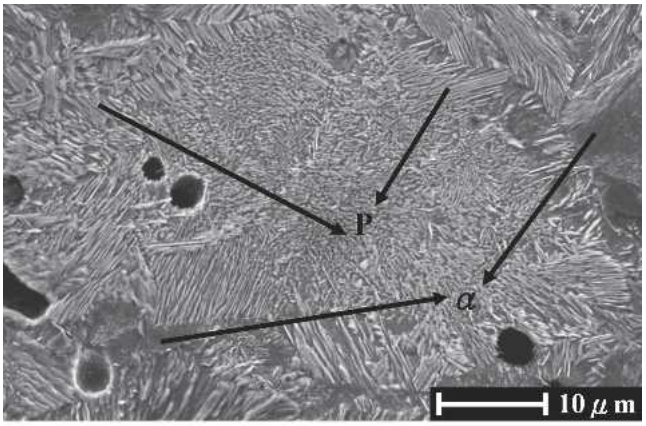

(*a*)

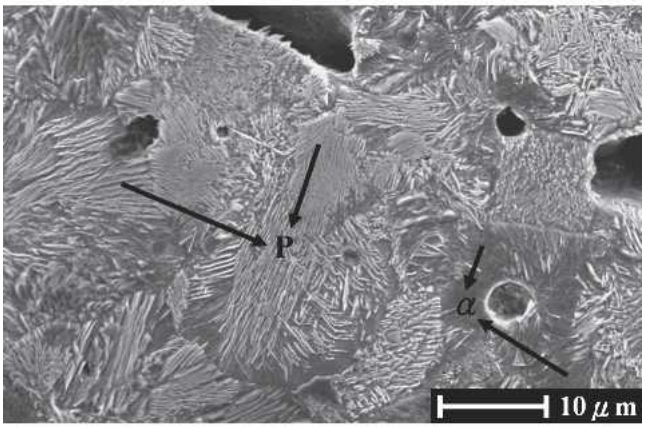

(*b*)

Fig. 2—The microstructures of the Fe-3Cr-0.5Mo-0.5C compacts that were sintered (*a*) at 1120 °C for 30 min and (*b*) at 1250 °C for 60 min.

diffusion into the matrix. When the Ni content in the powder interior was increased, the powder had a higher hardenability and thus it became more difficult for pearlite to form during cooling.

When the amount of added graphite increased, the microstructures of the FeCrMo-4Ni-0.6C compacts sintered at 1120 °C and 1250 °C, as shown in Figure 6, were similar to those containing 0.5 wt pct C. The Ni-rich austenite was still present and could be found even more easily than that in the FeCrMo-4Ni-0.5C specimen shown in Figure 3(a). This was possible because a higher carbon content lowers the martensite forming and finishing temperatures, M_s an M_f, significantly. Thus, the tensile strength and hardness decreased compared to those compacts containing 0.5 wt pct C.

To understand the exclusive effect of Cr in FeCrMo-4Ni material, Fe-0.5Mo-4Ni-0.5C (without 3.0 wt pct Cr) specimens were also prepared using Fe-0.5Mo prealloyed powders as the base material to which Ni and graphite powders were added. Figure 7 shows that the Fe-0.5Mo-4Ni-0.5C alloy sintered at 1120 °C contained a substantial amount of soft Ni-rich ferrite and austenite, which contained 3 to 5 and 13 to 25 wt pct Ni, respectively. These contents were very similar to the 3 to 5 and 11 to 23 wt pct Ni in the Ni-rich ferrite and austenite, respectively, in

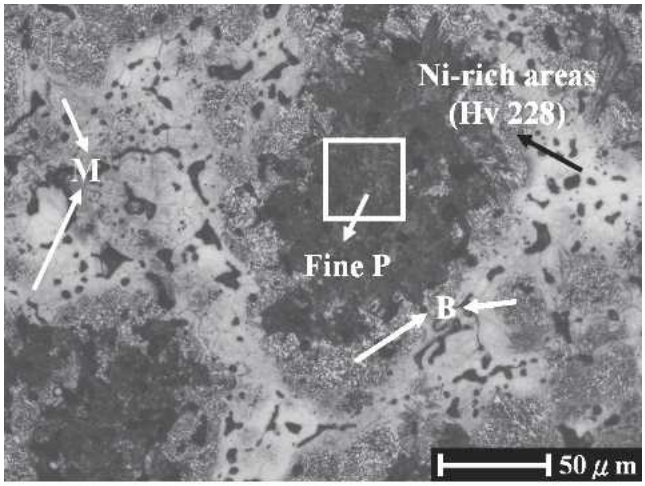

(*a*)

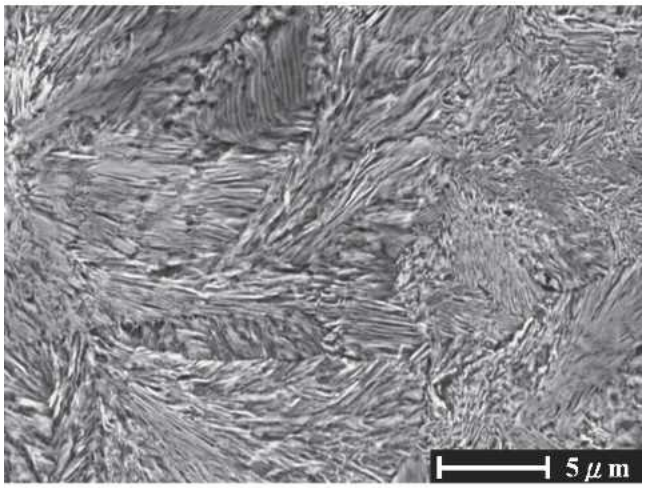

(*b*)

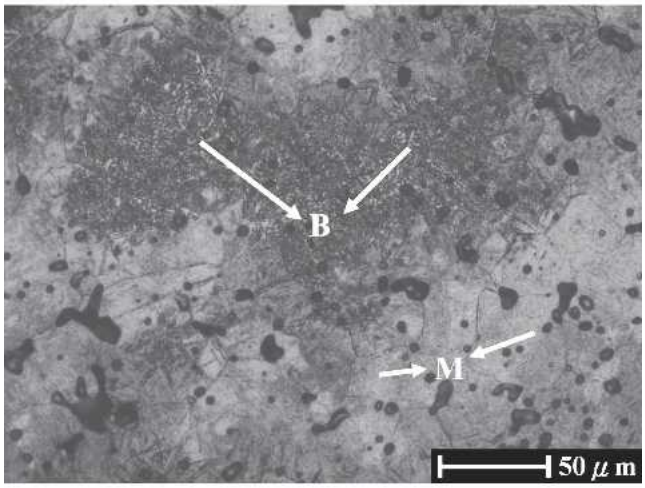

(*c*)

Fig. 3—The microstructures of the Fe-3Cr-0.5Mo-4Ni-0.5C compacts that were sintered (*a*) at 1120 °C for 30 min, (*b*) enlarged section of (a), and (*c*) at 1250 °C for 60 min.

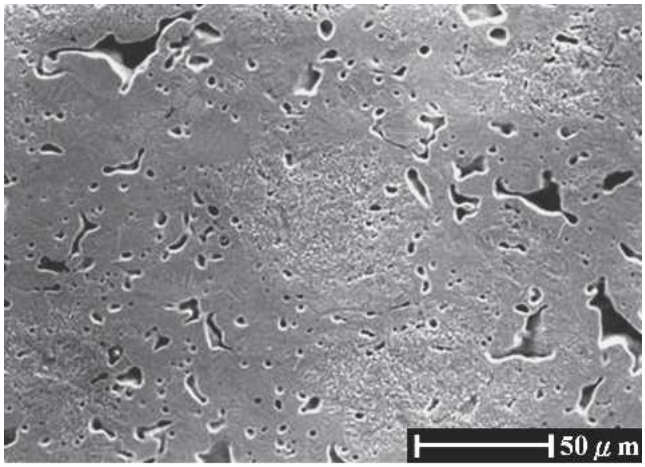

(*a*)

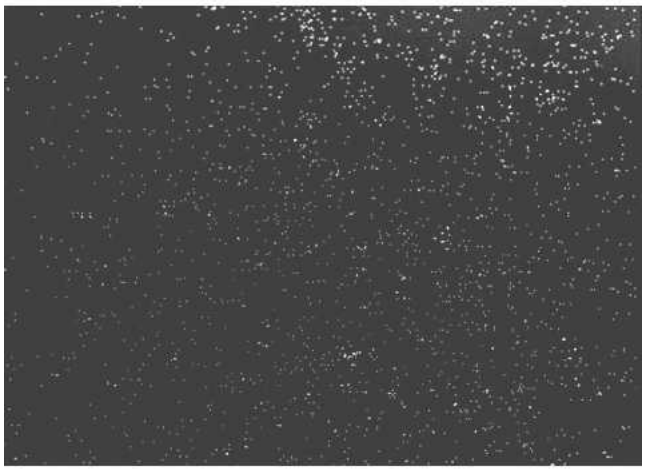

(*b*) Cr

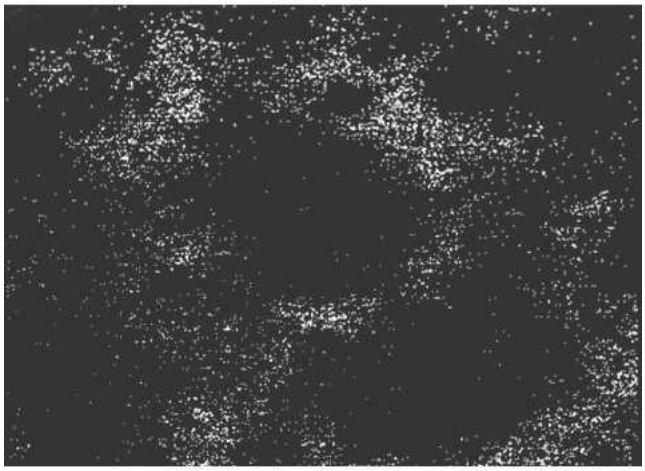

(*c*) Ni

Fig. 4—The Cr and Ni dot mappings of the Fe-3Cr-0.5Mo-4Ni-0.5C compact that was sintered at 1120 °C for 30 min.

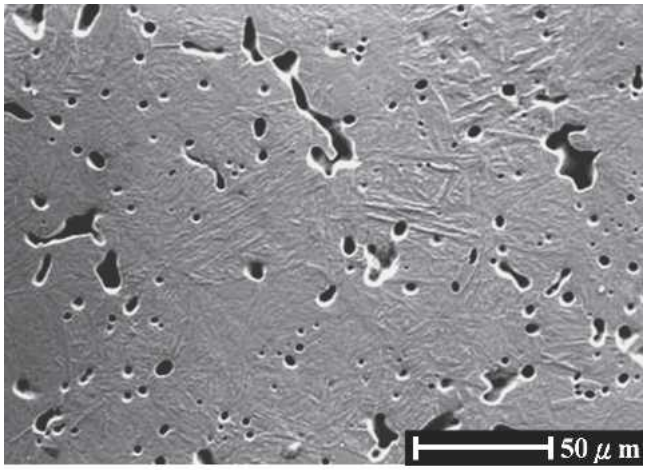

(*a*)

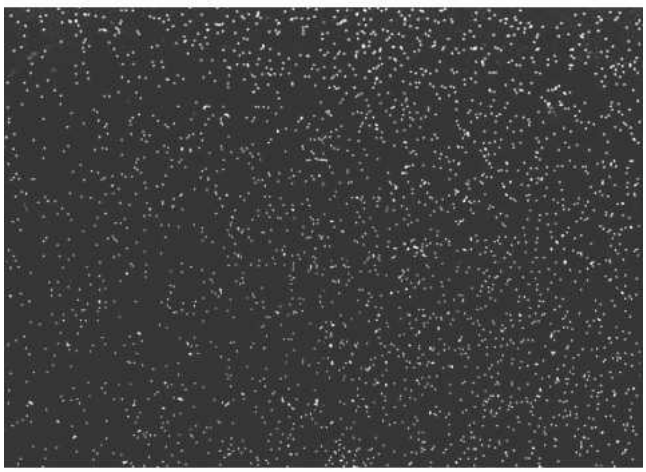

(*b*) Cr

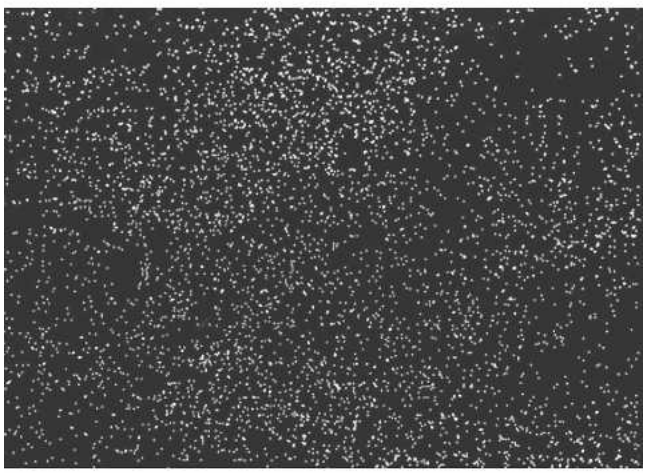

(*c*) Ni

Fig. 5—The Cr and Ni mappings of the Fe-3Cr-0.5Mo-4Ni-0.5C compact that was sintered at 1250 °C for 60 min.

the Fe-4Ni-0.5Mo-1.5Cu-0.5C steel, which was reported by Wu *et al.,* using the EBSD analysis.[2] These soft Ni-rich areas were not eliminated even after 1250 °C sintering. These soft areas were located either at powder peripheries or in pore-rich regions. It is believed that they result from the fast surface diffusion of Ni on iron powders and the slow inward diffusion of Ni into the iron matrix.[2,18]

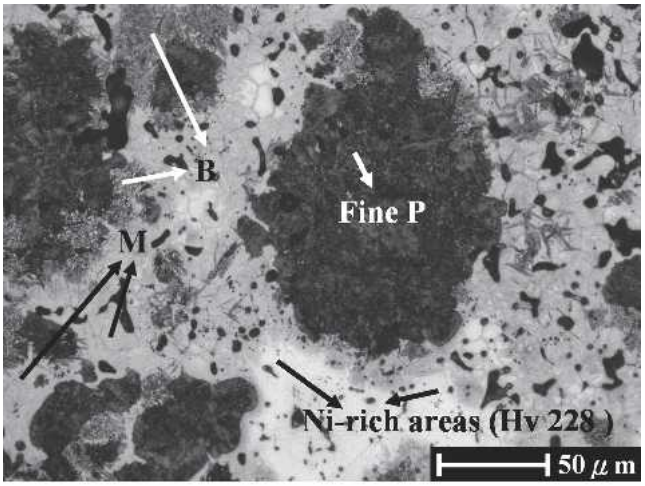

(*a*)

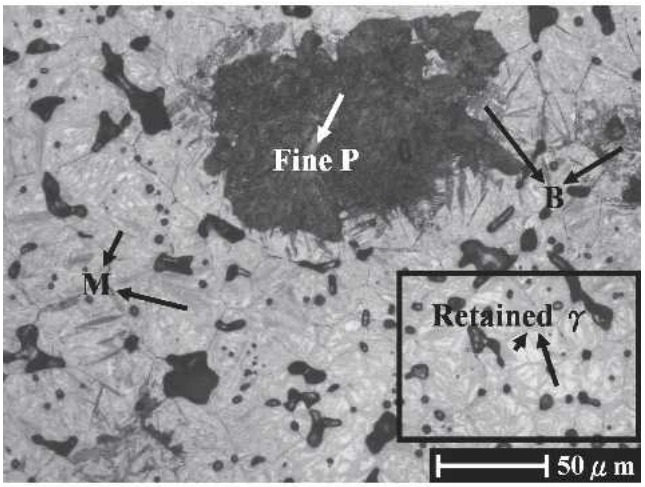

(*b*)

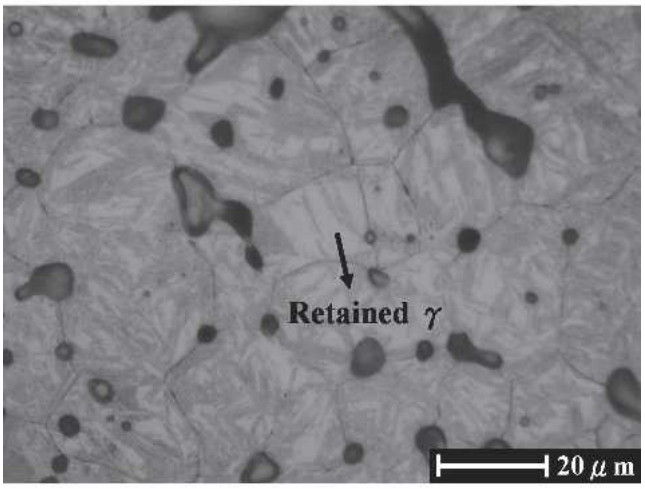

(*c*)

Fig. 6—The microstructures of the Fe-3Cr-0.5Mo-4Ni-0.6C compacts that were sintered (*a*) at 1120 °C for 30 min, (*b*) at 1250 °C for 60 min, and (*c*) enlarged section of (b).

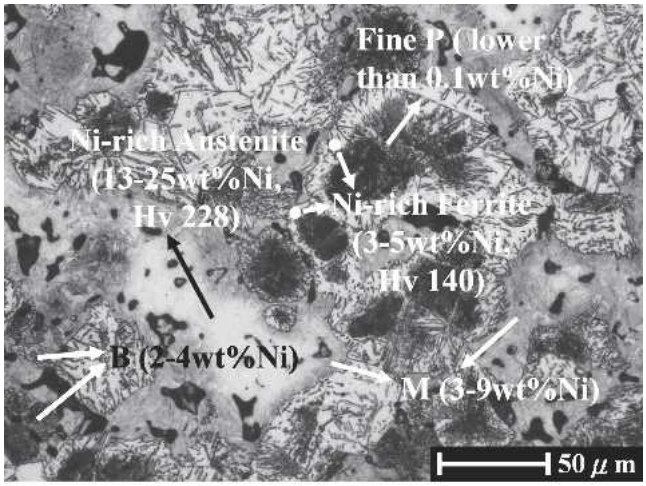

(*a*)

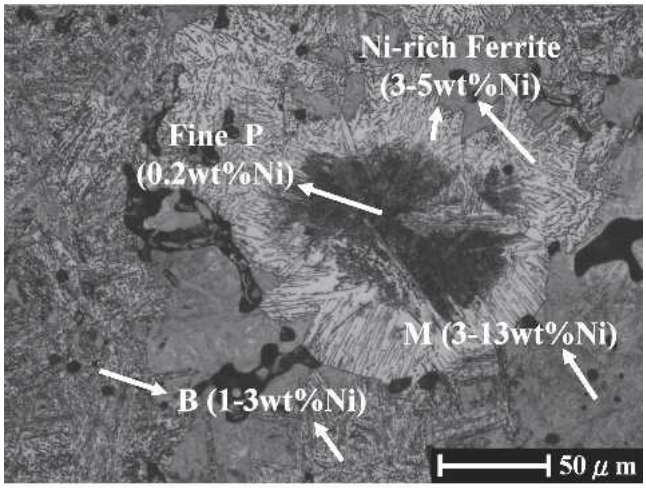

(*b*)

Fig. 7—The microstructures of the Fe-0.5Mo-4Ni-0.5C compacts that were sintered at (*a*) 1120 °C for 30 min and (*b*) 1250 °C for 60 min showing large amounts of Ni-rich areas.

Because these Ni-rich areas were near pores and were soft, these areas were prone to fracture. To verify that, the fracture path of the Fe-0.5Mo-4Ni-0.5C compact that was sintered at 1250 °C was examined inside an SEM. Figure 8 shows that the first typical fracture path is along the interface between Ni-rich ferrite and pearlite near pores and crossing the Ni-rich ferrite. Figure 9 shows the second typical fracture path, which crossed over the coarse pearlite in the center of iron powders. Both these fracture paths confirmed that the Ni-rich ferrite and pearlite, of which the strengths are inferior to those of bainite and martensite, are the vulnerable sites during mechanical testing and must be eliminated if the mechanical properties of this Fe-0.5Mo-4Ni-0.5C material need to be improved.

In contrast, Figure 3(c) shows no Ni-rich ferrite when 3 wt pct Cr is present. The Ni mapping of FeCrMo-4Ni-0.5C, as shown in Figure 5, also indicated a much better Ni distribution in the matrix. These comparisons confirmed that the improvement of the Ni distribution during sintering

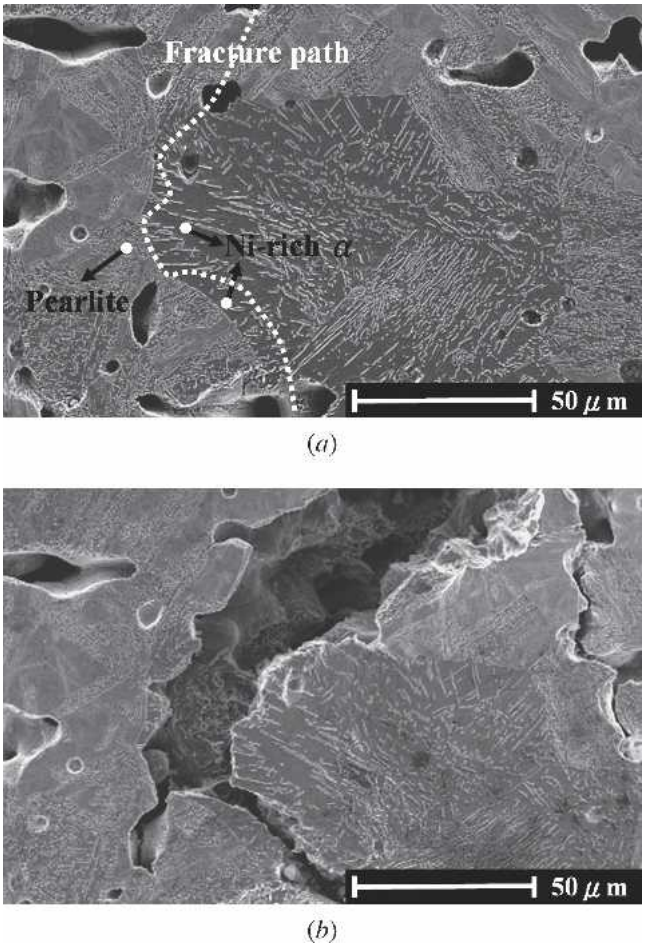

Fig. 8—The first typical fracture path in the sintered Fe-0.5Mo-4Ni-0.5C compact is along the interface between Ni-rich ferrite and pearlite near pores and crossing the Ni-rich ferrite: (*a*) before and (*b*) after fracturing.

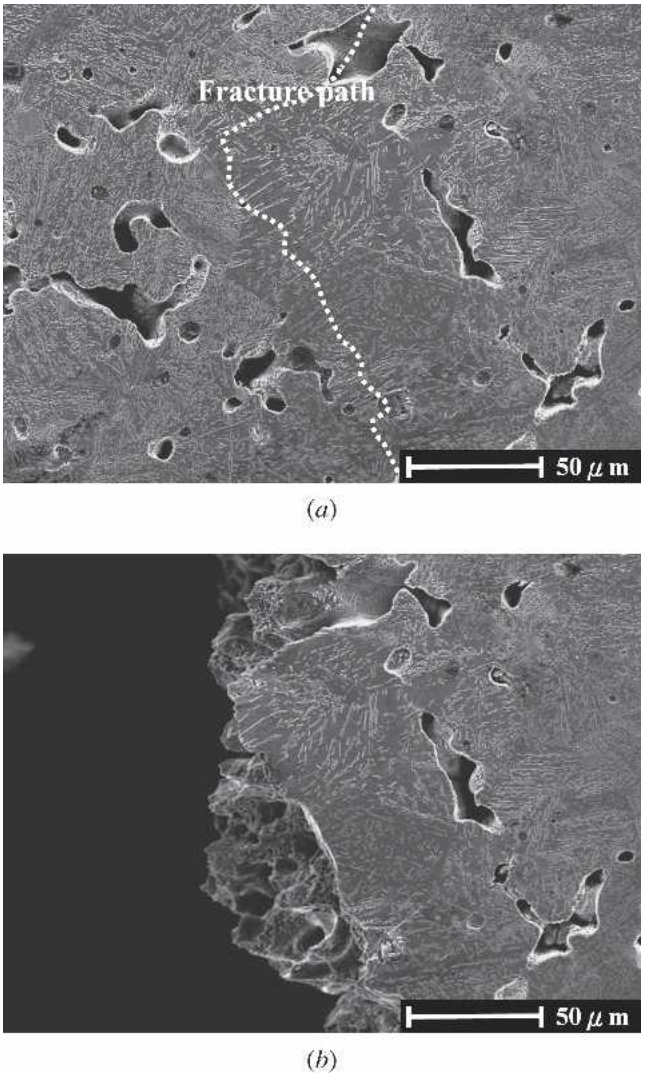

Fig. 9—The second typical fracture path in the sintered Fe-0.5Mo-4Ni-0.5C compact is to cross the coarse pearlite in the center of iron powders: (*a*) before and (*b*) after fracturing.

was mainly due to the Cr in the prealloyed powder, not the Mo.

D. *Thermodynamic Analysis*

The chemical potential of carbon in the Fe-0.5C-xNi, Fe-0.5Mo-0.5C-xNi, and Fe-3Cr-0.5Mo-0.5C-xNi steel compacts sintered at 1120 °C are shown in Figure 10, using the Thermo-Calc software. The calculations indicated that the chemical potential of carbon was increased with increasing Ni content for all three materials. This means that the Ni and C have a tendency to repel each other and cause carbon to diffuse out from Ni-rich areas.[2,12] With a low carbon and high Ni content, little bainite or martensite could be found in these Ni-rich/C-lean areas after cooling. However, the chemical potential of carbon in the Fe-0.5C-xNi compacts could be lowered slightly when 0.5 wt pct Mo was added and could be further reduced when 3 pct wt Cr was added. These results suggested that the addition of Cr could reduce the repelling effect sufficiently between nickel and carbon and decrease the degree of outward diffusion of carbon, thus keeping more carbon in the Ni-rich areas. As a consequence, more bainite and martensite should form at the expense of soft Ni-rich areas. These calculations are consistent with the microstructure observations, as indicated by a comparison between Figures 3 and 7.

IV. CONCLUSIONS

The Ni-containing PM steels contain a high portion of Ni-rich areas due to the poor homogenization of Ni. These Ni-rich areas were soft and were susceptible to fracture during mechanical testing, as was identified using an SEM. To attain a homogeneous microstructure, Fe-3Cr-0.5Mo prealloyed steel powders were employed in this study as the base material. The results show that the distribution of Ni and C was significantly improved compared to that of Cr-free materials. This was mainly due to the reduction of the repelling effect between carbon and nickel when Cr was present, as was indicated by the thermodynamic analysis results using the Thermo-Calc software. With a more homogeneous Ni and C distribution, more martensite and bainite were formed and most soft Ni-rich

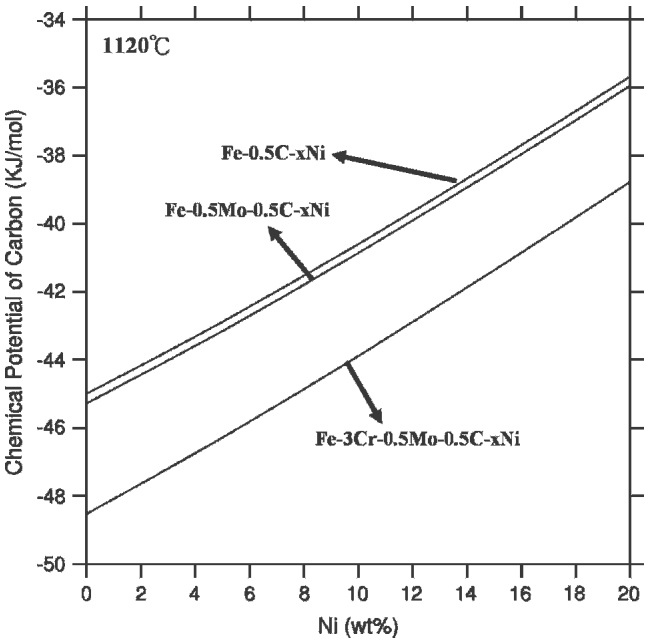

Fig. 10—The chemical potential of carbon in Fe-3Cr-0.5Mo-0.5C-xNi, Fe-0.5Mo-0.5C-xNi, and Fe-0.5C-xNi alloys shows that the addition of Cr could alleviate the strong repelling effect between Ni and C.

areas were eliminated. With an improved microstructure, the apparent hardness of the Fe-3Cr-0.5Mo-4Ni-0.5C compact was HRC 39.2, while the tensile strengths reached 1323 MPa. The elongation was greater than 1.0 pct. Despite the fact that these properties were obtained at a low sintered density of 7.23 g/cm^3 and a slow furnace cooling rate of 0.1 °C/s, these properties are comparable to those of sinter-hardened high-strength PM steels reported to date in the literature using accelerated cooling and are equivalent to those of the best quenched-and-tempered materials registered in the MPIF standards.

ACKNOWLEDGMENT

The authors thank the Lenco Co. and the National Science Council for their partial support of this project under Contract No. NSC 94-2622-E-002-008-CC3.

REFERENCES

1. *Materials Standards for P/M Structural Parts*, 2003 ed., Metal Powder Industries Federation, Princeton, NJ, pp. 42-49.
2. M.W. Wu, K.S. Hwang, H.S. Huang, and K.S. Narasimhan: *Metall. Mater. Trans. A*, 2006, vol. 37A, pp. 2559-68.
3. S. Carabajar, C. Verdu, A. Hamel, and R. Fougeres: *Mater. Sci. Eng.*, 1998, vol. 257A, pp. 225-34.
4. C. Verdu, S. Carabajar, G. Lormand, and R. Fougeres: *Mater. Sci. Eng.*, 2001, vols. 319A–321A, pp. 544-49.
5. N. Chawla and X. Deng: *Mater. Sci. Eng.*, 2005, vol. 390A, pp. 98-112.
6. W.A. Spitzig, R.E. Semlser, and O. Richmond: *Acta Metall.*, 1988, vol. 36 (5), pp. 1201-11.
7. R.J. Bourcier, D.A. Koss, R.E. Smelser, and O. Richmond: *Acta Metall.*, 1986, vol. 34 (12), pp. 2443-53.
8. S. T. Campbell, T. Singh, and F. Stephenson: *Advances in Powder Metallurgy & Particulate Materials*, compiled by W.B. James and R.A. Chernenkoff, eds., MPIF, Princeton, NJ, 2004, part. 7, pp. 105-15.
9. K.S. Hwang and M.Y. Shiau: *Metall. Mater. Trans. B*, 1996, vol. 27B, pp. 203-11.
10. H. Zhang and R.M. German: *Int. J. Powder Metall.*, 2002, vol. 38 (1), pp. 51-61.
11. B.A. Gething, D.F. Heaney, D.A. Koss, and T.J. Mueller: *Mater. Sci. Eng.*, 2005, vol. 390A, pp. 19-26.
12. A.L. Sozinov and V.G. Gavrilijuk: *Scripta Mater.*, 1999, vol. 41 (6), pp. 679-83.
13. P. Ortiz and F. Castro: *Powder Metall.*, 2004, vol. 47 (3), pp. 291-98.
14. T. Marcu, A. Molinari, G. Straffelini, and S. Berg:. *Powder Metall.*, 2005, vol. 48 (2), pp. 139-43.
15. B. Hu, A. Klekovkin, D. Milligan, and U. Engstrom: *Advances in Powder Metallurgy & Particulate Materials*, compiled by W.B. James and R.A. Chernenkoff, MPIF, Princeton, NJ, 2004, part 7, pp. 28-40.
16. F. Hanejko, A. Taylor, and A. Rawlings: *Advances in Powder Metallurgy & Particulate Materials*, compiled by V. Arnhold, C.L. Chu, W.F. Jandeska, and H.I. Sanderow, MPIF, Princeton, NJ, 2002, part 13, pp. 35-47.
17. M. Youseffi, C.S. Wright, and F.M. Jeyacheya: *Powder Metall.*, 2002, vol. 45 (1), pp. 53-62.
18. J. Puckert, W.A. Kaysser, and G. Petzow: *Int. J. Powder Metall.*, 1984, vol. 20 (4), pp. 301-10.